Progress In Electromagnetics Research, PIER 77, 243–266, 2007

LINEAR AND NONLINEAR SUPERIMPOSED BRAGG GRATING: A NOVEL PROPOSAL FOR ALL-OPTICAL MULTI-WAVELENGTH FILTERING AND SWITCHING

H. Ghafoori-Fard and M. J. Moghimi

Faculty of Electrical Engineering
Amirkabir University of Technology
Tehran, Iran

A. Rostami

Photonics and Nanocrystal Research Lab.
Faculty of Electrical and Computer Engineering
University of Tabriz
Tabriz 51664, Iran

Abstract—In this paper, the linear and nonlinear applications including optical filtering and switching of superimposed Bragg grating are presented. For realization of superimposed Bragg grating electro-optic effect is used. The introduced system acts as an optical chip. The induced superimposed index of refractions due to sampled electric potentials applied through metallic strips on electro-optically active core-cladding are investigated analytically and simulated numerically using the Transfer Matrix Method (TMM). It is shown that the applied electric field induces superimposed refractive index grating, which can be controlled using amplitudes and frequency contents of potential samples as well as optical waveguide parameters. Our proposed structure is analog programmable device for realization of many interesting optical signal conditioners such as optical filters, optical beam splitters, and many other special transfer functions in linear case. The proposed device is tunable and can be controlled using the applied potential parameters (samples) and easily satisfy dense wavelength division multiplexing (DWDM) system demand specifications. The electro-optic Pockels effect for generation of the superimposed gratings in this building block will be used. Then we propose an optical chip for performing the introduced functions. In practical cases, for realization of DWDM demands, we need very large number of potential samples approximately 3 to 4 orders of magnitudes. So, this type of block

as optical controllable chip really from practical point of views is impossible and illegal. In this paper, we will present a simple approach for decreasing the number of efficient control samples from outside for managing the proposed tasks. Our calculations in this paper shows that with less than approximately 200 control pins, we can realize all of proposed practical ideas with acceptable precision. Also, with 3 samples per period, our design will cover 215 individual DWDM channels theoretically from 1.55 um towards lower wavelengths and 325 channels for 4 samples per period case, which is infinity from practical point of views. All of transfer functions corresponding to these channels can be manipulated using applied potential samples.

Also, as nonlinear applications of the superimposed Bragg grating multi-wavelength optical switching is presented. For this purpose the switching operation is illustrated first and then switching thresholds in the case of three predefined wavelengths are shown. Thus we illustrate numerical results for demonstration of the ability of the proposed structure. At the same time, we investigate effects of the parameters of the proposed structure such as the nonlinear refractive index and the grating length (number of layers) on switching performance including threshold intensity and slope of transition function. The proposed structure can be used as multi-wavelength switching applicable to DWDM and multi wavelength communication systems.

1. INTRODUCTION

Dense wavelength division multiplexing (DWDM) has been widely used as a method of expanding the capacity of optical fiber networks. This type of optical communication techniques needs some basic blocks with capabilities including multiplexing, demultiplexing, switching, routing monitoring and attenuation of each individual wavelength within the packet of wavelengths propagating through optical fiber network. These functions can be realized with passive components, which there are interesting and currently used for optical signal processing. In optical passive devices the Bragg Gratings is widely used, discussed in literature and applied for optical signal processing tasks [1–3]. Usually, these devices can be implemented using Bragg Gratings. Nowadays, from our point of view, these functions are implemented separately (single function passive device) without efficient controllable and reconfigurable algorithm in electrical (electro-optical functional blocks) and optical domains (all-optical functional blocks). So, if optical devices can be integrated into electronically controllable geometry there will be a basis for the programmable optical functional

devices. These types of devices really are new and can be useful for more development of optical processing and computing with flexible programming. So, there is basic interest for introducing and development of the mentioned devices and systems for realization of optical computing.

There are some published papers, which are related to the way how these structures (electro-optical) can be analyzed and implemented. For example, Kulishov [4–9] presented some papers on interdigitated electrode-induced phase gratings using electrical signals in recent years. In these papers, he tries to show that using a large number of periodic interdigitated metallic electrodes with alternating applied different sign and constant potentials, the superimposed (two transmission curves only) and tunable gratings can be obtained. His research was limited on two transmission curves only without control on each transmission curves separately. In these works, the applied electric field as control signal is superposition of two basic fields with different periods. So, two transmission curves do not have similar characteristics, because these two basic fields have different periods (the period of second field is twice of the first one). But, in practice, especially for DWDM applications, we need more than two transmission or reflection curves with separately controllable characteristics, which based on this research is impossible. His theoretical background is based on Glytsis et al. [10] work, which is an especial case with analytical solution for the Laplace equation and is good method for evaluation of the interdigitated electrodes electro-optical systems.

So, in this paper, we try to present a general method for realization of electronically controllable reflection or transmission curves satisfying DWDM demands and including a large number of selective individual channels simultaneously, which is impossible using Kulishov presented method. Our method is based on suitable (depending on how many channels will be covered) encoding of the superimposed continuous potential applied on metallic layers in electro-optically active waveguide. With selection of suitable number of samples per period, really very large (practically infinite) number of DWDM channels can be covered in this system. But, for implementation of this idea, we need more strips for application of potential, which in this problem probably looks impractical. So, for lowering the number of strips as control pins to be in logical situation, which is due to sampling effect, approximation techniques will be used. In this case, we apply same potential to some adjacent strips with considering phase relations. So, from user point of view, the optical chip should have small number of control pins. Then, based on our proposed technique, we will propose an optical chip with less than 200

control pins for realization of all proposed purposes. Also, this building block can be very useful basis for implementation of most necessary tasks in optical and especially DWDM networks with reconfigurability and programmable capability.

Finally the proposed structure can be operated as optical switch. Some interesting proposals for optical switching were presented so far. Especially fast optical single and multi wavelength switching is critical element in high speed communications and computing. Also, the unprecedented demand for optical network capacity has fueled the development of long-haul optical network systems which employ wavelength-division multiplexing (WDM) to achieve tremendous capacities. Up to now, the switching burden in such systems has been laid almost entirely on electronics. Electronic switching is a mature and sophisticated technology that has been studied extensively. However, as the network capacity increases, electronic switching nodes seem unable to keep up. Apart from that, electronic equipment is strongly dependent on data rate and protocol. If optical signals could switch without conversion to electrical form, both of these drawbacks would be eliminated. The transfer of the switching function from electronics to optics will result in a reduction in the network equipment, an increase in the switching speed, and thus network throughput, and a decrease in the operating power. Some of the most popular applications of optical switches consist of optical cross-connects [11], optical Add/Drop multiplexing [12], optical signal monitoring.

Many schemes have been suggested for all optical switching, for example by using nonlinear loop mirror, nonlinear directional coupler [13], Liquid-crystal optical switches [14, 15], Semiconductor Optical Amplifier Switches (SOAs) [11, 16] and nonlinear grating [17–19]. In some of theses designs, such as SOAs or electro-optic switches still need electronic devices to operate. In some others like nonlinear Bragg gratings switching more than one input frequency needs cascade switches with different band-pass. Kerr-like nonlinearity in periodic, quasi-periodic and aperiodic structures has been used for switching purposes also [20–28]. In these references different aspects of periodic structures have been considered using spectral tools and scattering parameters. But, in the presented papers there isn't a design methodology for multi-wavelength filtering and switching. So, in this paper, we propose a complex nonlinear grating that can switch different input wavelengths at the same time.

Organization of the paper is as follows.

In Section 2 mathematical background is introduced. Electro-optically induced superimposed Bragg Grating is discussed in Section 3. In Section 4 simulation results are presented and discussed.

Finally the paper ends with a short conclusion.

2. MATHEMATICAL BACKGROUND

For multi wavelength optical switching the following proposal is considered (Fig. 1). In this figure a thick substrate and a thin optical complex multilayer generally including different index of refractions and layer thicknesses is considered as an optical multi wavelength filters and switches. In the proposed structure predefined wavelengths at given intensity reflected back from the structure and using different optical methods each wavelength can be separated to desired positions at different nodes. For this structure the index of refraction generally can be explained as follows.

$$n(x) = n_{ave} + \sum_{i=1}^{m} \delta_l \sin(k_i x) \; - \left|E^2\right| \sum_{i=1}^{m} \delta_{nl} \sin(k_i x), \qquad k_i = \frac{2\pi}{\Lambda_i} \tag{1}$$

where n_{ave}, δ_l, δ_{nl}, Λ_i and E are average index of refraction, amplitude of the index of refraction for lth linear grating, amplitude of the nonlinear grating, period of grating and electric field respectively.

To analyze this structure, we divided it into N sections. Each section is considered homogenous. The approximated multilayer

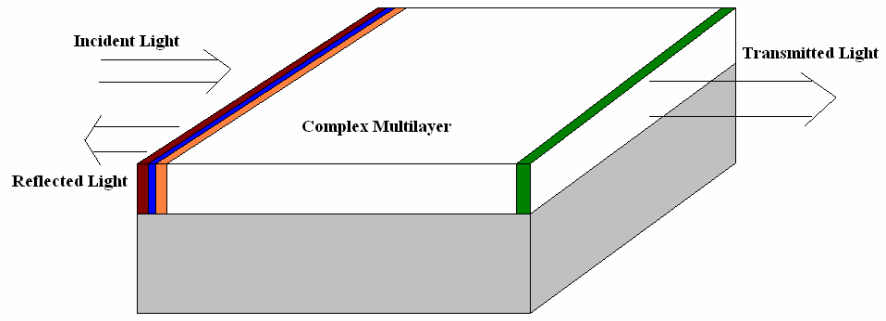

Figure 1. Schematic of the proposed multi wavelength optical switch.

dielectric structure is described by

$$n(x) = \begin{cases} n_0 & x < x_0 \\ n_1 & x_0 < x < x_1 \\ n_2 & x_1 < x < x_2 \\ . & \\ . & \\ n_N & x_{N-1} < x < x_N \\ n_s & x_N < x \end{cases}, \tag{2}$$

where n_l, x_l, n_s and n_0 are the refractive index of lth layer, the position of the interface between the lth layer and the $(l+1)$th layer, the substrate index of refraction and the incident medium respectively. The layer thicknesses d_i are L/N, where L is the length of the grating.

$$d_i = \frac{L}{N}, \quad i = 1, 2, 3, \ldots, N \tag{3}$$

The electric field of a general plane-wave solution of the wave equation can be written as:

$$E = E(x)e^{i(\omega t - \beta z)}, \tag{4}$$

where the electric field distribution $E(x)$ can be written as

$$E(x) = \begin{cases} A_0 e^{-ik_{0x}(x-x_0)} + B_0 e^{ik_{0x}(x-x_0)} & x < x_0 \\ A_l e^{-ik_{lx}(x-x_l)} + B_l e^{ik_{lx}(x-x_l)} & x_{l-1} < x < x_l \\ A_s e^{-ik_{sx}(x-x_N)} + B_s e^{ik_{sx}(x-x_N)} & x_N < x \end{cases}, \tag{5}$$

where k_{lx} is the x component of wave vectors given as follows.

$$k_{lx} = \left[\left(\frac{n_l \omega}{c} \right)^2 - \beta^2 \right]^{\frac{1}{2}} \tag{6}$$

Also, it is related to the incident ray angle θ_l as

$$k_{lx} = n_l \frac{\omega}{c} \cos(\theta_l) = \frac{2\pi}{\lambda} \cos(\theta_l) \tag{7}$$

The electric field $E(x)$ consists of forward and backward traveling wave and can be defined in the following form.

$$E_l(x) = \mathrm{Re}^{-ik_l x} + Le^{ik_l x} = A_l(x) + B_l(x) \tag{8}$$

where $\pm k_l x$, R and L are constants in homogenous layer. $E(x)$ is a continuous function of x. Using the transfer matrix method the following relations are used for connection of the field amplitudes in different layers as follows.

$$\begin{pmatrix} A_0 \\ B0 \end{pmatrix} = D_0^{-1} D_l \begin{pmatrix} A_l \\ B_l \end{pmatrix} \tag{9}$$

$$\begin{pmatrix} A_l \\ B_l \end{pmatrix} = P_l D_l^{-1} D_{l+1} \begin{pmatrix} A_{l+1} \\ B_{l+1} \end{pmatrix}, \tag{10}$$

where A_l and B_l represent the amplitude of plane waves at interface $x = x_l$ and D_l is dynamic matrix described as follows.

$$D_\alpha = \begin{pmatrix} 1 & 1 \\ n_\alpha \cos\theta_\alpha & -n_\alpha \cos\theta_\alpha \end{pmatrix}, \quad \alpha = 0, l, l+1, \tag{11}$$

where θ_α is the incident ray angle in each layer. Also, P_l is propagation matrix and defined by:

$$P_l = \begin{pmatrix} e^{i\phi_l} & 0 \\ 0 & e^{-i\phi_l} \end{pmatrix}, \tag{12}$$

where

$$\phi_l = k_{lx}.d_l. \tag{13}$$

The relation between A_0, B_0, A_s and B_s (or A_{N+1}, B_{N+1}) can be determined finally as

$$\begin{pmatrix} A_0 \\ B_0 \end{pmatrix} = \begin{pmatrix} M_{11} & M_{12} \\ M_{21} & M_{22} \end{pmatrix} \begin{pmatrix} A_s \\ B_s \end{pmatrix}, \tag{14}$$

where the matrix M given as follows.

$$\begin{pmatrix} M_{11} & M_{12} \\ M_{21} & M_{22} \end{pmatrix} = D_0^{-1} \left[\prod_{i=1}^{N} D_i P_i D_i^{-1} \right] D_s \tag{15}$$

This approach is named Transfer Matrix Method (TMM). If the incident light comes from medium 0, the reflection coefficient is defined as:

$$r(\lambda) = \left(\frac{B_0}{A_0} \right)_{B_s = 0} \tag{16}$$

Similarly, the transmission coefficient is:

$$t(\lambda) = \left(\frac{A_s}{A_0}\right)_{B_s=0} \tag{17}$$

Using Eq. (14) and definitions presented in Eqs. (15) and (16), we obtain:

$$r(\lambda) = \frac{M_{21}}{M_{11}} \tag{18}$$

and

$$t(\lambda) = \frac{1}{M_{11}}. \tag{19}$$

Reflectance of the proposed structure is given as follows provided that the incident medium is lossless.

$$R(\lambda) = |r(\lambda)|^2 = \left|\frac{M_{21}}{M_{11}}\right|^2 \tag{20}$$

3. ELECTRO-OPTICALLY INDUCED SUPERIMPOSED GRATINGS

The electro-optical system to be analyzed is demonstrated in Fig. 2. As it is shown, T and d are the optical waveguide and buffer layer thickness respectively. Layer 1 and 5 are superstrate and substrate respectively and is extended to infinity. Between superstrate, substrate

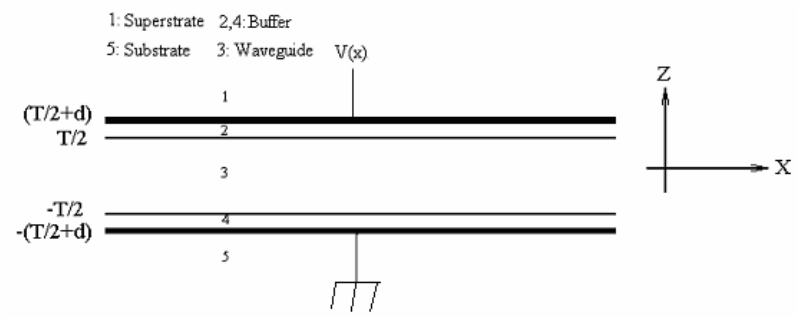

Figure 2. Schematics of electro-optically induced reconfigurable waveguide gratings.

and buffer layers two thin metallic layers with high conductivity (for ignoring from metallic layers thickness in analysis) are used for potential application and grounding. Buffer layers are used for minimizing the optical signal loss. Waveguide and Buffer layers are electro-optical materials and anisotropic. Also, the cladding region can use isotropic matter, which in optical chip section it is assumed. Thus, their principal axis are aligned along the x and the z directions such that the dielectric properties can be described by two diagonal relative permittivities $\varepsilon_{xx}^{Co}, \varepsilon_{zz}^{Co}$ and $\varepsilon_{xx}^{Cl}, \varepsilon_{zz}^{Cl}$ for the core and the cladding respectively. Metallic layers in y-direction are long and in this situation, we can consider two-dimensional case for potential distribution. Also, in the x-direction metallic layers are extended very large compared to waveguide thickness (T) and we can ignore the end boundary effects. Finally, we accept that potential distribution can be assumed to be electrostatic (for steady state analysis) because of low frequency nature of potential compared optical signal frequency variation inside waveguide.

The electrostatic nature of the analysis permits association of an electric potential $\Psi^{(i)}(x,z)$ with each region i ($i = 1, 2, 3, 4, 5$), and the two-dimensional Laplace equation can be written for each region i as

$$\varepsilon_{xx}^{(i)} \frac{\partial^2 \Psi^{(i)}(x,z)}{\partial x^2} + \varepsilon_{zz}^{(i)} \frac{\partial^2 \Psi^{(i)}(x,z)}{\partial z^2} = 0, \tag{21}$$

where $\varepsilon_{xx}^{(i)}$ and $\varepsilon_{zz}^{(i)}$ are the two diagonal permittivities of region i. The layers i are defined as

$$\begin{aligned}
\left(\frac{T}{2} + d\right) \le Z \le \infty, \quad & i = 1, \\
\left(\frac{T}{2}\right) \le Z \le \left(\frac{T}{2} + d\right), \quad & i = 2, \\
\left(-\frac{T}{2}\right) \le Z \le \left(\frac{T}{2}\right), \quad & i = 3, \\
-\left(\frac{T}{2} + d\right) \le Z \le -\left(\frac{T}{2}\right), \quad & i = 4, \\
-\infty \le Z \le -\left(\frac{T}{2} + d\right), \quad & i = 5.
\end{aligned} \tag{22}$$

The symmetry of the proposed structure and the following boundary conditions can be used for obtaining the constants in the

proposed solution for the Laplace equation.

$$\begin{aligned}
&\Psi^{(2)}\left(x, z = \pm\left(\frac{T}{2} + d\right)\right) = V(x), 0,\\
&\Psi^{(2)}\left(x, z = \frac{T}{2}\right) = \Psi^{(3)}\left(x, z = \frac{T}{2}\right),\\
&\Psi^{(3)}\left(x, z = -\frac{T}{2}\right) = \Psi^{(4)}\left(x, z = -\frac{T}{2}\right),\\
&\varepsilon_{zz}^{Cl}\frac{\partial\Psi^{(2)}\left(x, z = \frac{T}{2}\right)}{\partial z} = \varepsilon_{zz}^{Co}\frac{\partial\Psi^{(3)}\left(x, z = \frac{T}{2}\right)}{\partial z},\\
&\varepsilon_{zz}^{Cl}\frac{\partial\Psi^{(4)}\left(x, z = -\frac{T}{2}\right)}{\partial z} = \varepsilon_{zz}^{Co}\frac{\partial\Psi^{(3)}\left(x, z = -\frac{T}{2}\right)}{\partial z}.
\end{aligned} \tag{23}$$

By defining the new variable $u = \sqrt{\frac{\varepsilon_{xx}^{(i)}}{\varepsilon_{zz}^{(i)}}}z$, the simple form of the Laplace equation is obtained as follows.

$$\frac{\partial^2\Psi^{(i)}(x,z)}{\partial x^2} + \frac{\partial^2\Psi^{(i)}(x,u)}{\partial u^2} = 0. \tag{24}$$

Also, the boundary conditions can be converted in terms of the proposed new variable. The general solution for the Laplace equation in this form is usually given as follows.

$$\Psi^{(i)}(x,u) = \int_{-\infty}^{\infty}[A(k)e^{-ku} + B(k)e^{ku}]e^{ikx}, \tag{25}$$

where $A(k)$ and $B(k)$ are constants, which are related to boundary conditions and really are the Fourier transform of initial potential distributed in x-direction and applied to metallic layers at $U = 0$. In periodic cases (periodic interdigitated metallic fingers [4–9]), the integration can be reduced to single frequency and summation on harmonics, similar to Fourier series expansion of applied square wave potential [10]. But, in our case, we like investigating only the first harmonics of potential distribution (first terms of this expansion) because this part of potential through Pockels electro-optical effect and coupled mode differential equations can play a critical role in our calculations. In our case, there might be many frequency components (different frequency components not harmonics) in applied potential in

the continuous or sampled forms (superimposed signal case $V_{in}(x) = \sum_{j=-N}^{N} V_j \sin(k_j x)$). For including this matter into the Laplace equation solution, we assume that there are $2N+1$ discrete and different frequency components (band limited case) in the applied potential. So, in the following, we try to present a solution for the Laplace equation including band limited applied potential.

$$\Psi^{(1)}(x,z) = \sum_{j=-N}^{N} C_j e^{-k_j z} \sin(k_j x), \tag{26}$$

$$\Psi^{(2)}(x,z) = \sum_{j=-N}^{N} \left[A_j \cosh\left(k_j \delta_2 \left(z - \frac{T}{2}\right)\right) + B_j \sinh\left(k_j \delta_2 \left(z - \frac{T}{2}\right)\right)\right] \sin(k_j x), \tag{27}$$

$$\Psi^{(3)}(x,z) = \sum_{j=-N}^{N} \left[D_j \sinh\left(k_j \delta_3 z\right) + E_j \cosh\left(k_j \delta_3 z\right)\right] \sin\left(k_j x\right), \tag{28}$$

$$\Psi^{(4)}(x,z) = \sum_{j=-N}^{N} \left[F_j \cosh\left(k_j \delta_2 \left(z + \frac{T}{2}\right)\right) + G_j \sinh\left(k_j \delta_2 \left(z + \frac{T}{2}\right)\right)\right] \sin\left(k_j x\right), \tag{29}$$

$$\Psi^{(5)}(x,z) = \sum_{j=-N}^{N} H_j e^{+k_j z} \sin(k_j x), \tag{30}$$

where $\delta_2 = \sqrt{\frac{\varepsilon_{xx}^{Cl}}{\varepsilon_{zz}^{Cl}}}$, $\delta_3 = \sqrt{\frac{\varepsilon_{xx}^{Co}}{\varepsilon_{zz}^{Co}}}$, k_j and $2N+1$ are the respected wave vectors corresponding to frequency contents of applied potential and the number of superimposing components respectively. Now, we should apply the boundary conditions for determination of the constants in the proposed solution. Since the application of continuous potential in practice is very hard and impossible using traditional existing technologies, so, we try to sample (discretization) and the samples are applied through metallic layers with practical (realizable) distances (Fig. 3). So, based on this idea, we have many metallic strips (for satisfying sampling theory) on buffer layers and these strips encode the continuous potential into discrete form. This idea will be excellent for creating many superimposed gratings without changing the physics of design. Thus, based on Fig. 3, the superimposed gratings

for all DWDM applications and many others optical transfer functions needed for optical processing and conditioning can be implemented with constant geometry and only with changing the applied potential waveform. Thus, our proposed device is really analog programmable block in optical domain. The potential waveforms depends on what operation should be performed can be determined exactly.

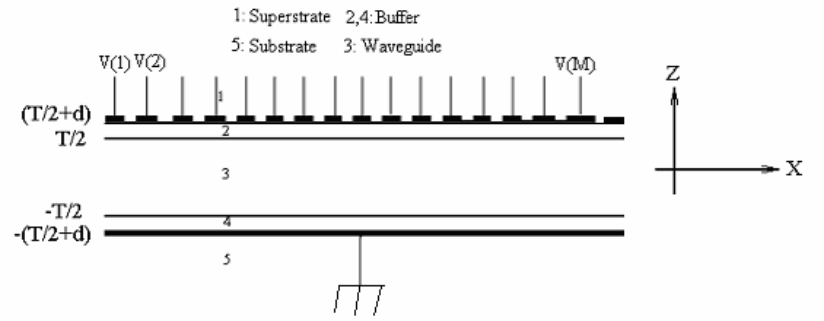

Figure 3. Sampled continuous potential through discrete strips.

Now, with applying the boundary conditions on proposed solution (Eqs. (26)–(30)), the following relations between constants can be obtained as

$$
\begin{aligned}
H_j &= 0,\\
C_j &= e^{k_j(T/2+d)}V_j,\\
B_j &= \eta\left[D_j\cosh\left(k_j\delta_3\frac{T}{2}\right)+E_j\sinh\left(k_j\delta_3\frac{T}{2}\right)\right], \qquad (31)\\
A_j &= \left[D_j\sinh\left(k_j\delta_3\frac{T}{2}\right)+E_j\cosh\left(k_j\delta_3\frac{T}{2}\right)\right],\\
F_j &= \tanh(k_j\delta_2 d)G_j,\\
F_j &= \left[-D_j\sinh\left(k_j\delta_3\frac{T}{2}\right)+E_j\cosh\left(k_j\delta_3\frac{T}{2}\right)\right], \qquad (32)\\
G_j &= \eta\left[D_j\cosh\left(k_j\delta_3\frac{T}{2}\right)-E_j\sinh\left(k_j\delta_3\frac{T}{2}\right)\right],\\
E_j &= \gamma D_j, \qquad (33)\\
D_j &= \frac{V_j}{\zeta_1\cosh(k_j\delta_2 d)+\eta\zeta_2\sinh(k_j\delta_2 d)}, \qquad (34)
\end{aligned}
$$

where $\zeta_1 = \sinh(k_j\delta_3\frac{T}{2}) + \gamma\cosh(k_j\delta_3\frac{T}{2})$, $\zeta_2 = \cosh(k_j\delta_3\frac{T}{2}) +$

$\gamma \sinh(k_j \delta_3 \frac{T}{2})$, $\eta = \frac{\varepsilon_{zz}^{Co}}{\varepsilon_{zz}^{Cl}} \frac{\delta_3}{\delta_2}$, and $\gamma = \frac{\sinh(k_j \delta_3 \frac{T}{2}) + \eta \tanh(k_j \delta_2 d) \cosh(k_j \delta_3 \frac{T}{2})}{\cosh(k_j \delta_3 \frac{T}{2}) + \eta \tanh(k_j \delta_2 d) \sinh(k_j \delta_3 \frac{T}{2})}$.

If we consider the sampled potential applied at $(\frac{T}{2} + d)$ into the proposed solution, the constants V_j can be determined based on Discrete Fourier transform of the applied potential samples through metallic strips ($Potential - Samples$, $V_{in}(n) \rightarrow DFT \rightarrow V_j$).

If we consider M potential samples applied on metallic layers, the following formula, which is Discrete Fourier Transform, can be used for determination of the constants V_j.

$$V(n) = \frac{1}{M} \sum_{m=0}^{M-1} V_{in}(m) e^{-i2\pi nm/M}, \tag{35}$$

where $V_{in}(m)$ are potential samples.

Finally, all of other coefficients appearing in the Laplace solution can be determined using Eq. (35) and Eqs. (31)–(34). Fig. 4 shows the typical potential distribution in the suprestrate (a), cladding (b, d) and core (c) regions respectively for typical simulating parameters values. In this simulation, we consider 5 frequency components corresponding to DWDM channels centered on 1.55 um with same amplitudes 10. For the thick core and cladding regions for obtaining the same result for the field and index of refraction distributions, one should apply higher potential amplitude. Using potential amplitude and optical waveguide parameters, we can engineer the induced index of refraction distribution.

As it is shown in the presented simulation result and slow variation of hyperbolic functions for thin core, using core and cladding regions parameters the potential distribution in the core can be approximated as linear function versus Z direction. So, we can imagine that field distribution only depends on X-direction and we have one-dimensional problem really. So, all developed techniques for one-dimensional Gratings can be applied in this case. In the following one-dimensional analysis is presented for our proposal.

Figure 5 shows the potential distribution inside core region including five DWDM channels with equal amplitudes ($V_j = 10$) for medium approximately 3 mm length. This figure clearly illustrates superposition of harmonic functions, which can be related to superimposed Bragg gratings using electro-optical Pockels effect.

Now, the electric field distribution in the x and z directions can be calculated based on obtained potential distribution and the following

relations.

$$E_x^{(i)}(x,z) = -\frac{\partial \Psi^{(i)}(x,z)}{\partial x},$$
$$E_z^{(i)}(x,z) = -\frac{\partial \Psi^{(i)}(x,z)}{\partial z}. \tag{36}$$

So, the following relations can be considered as electric field

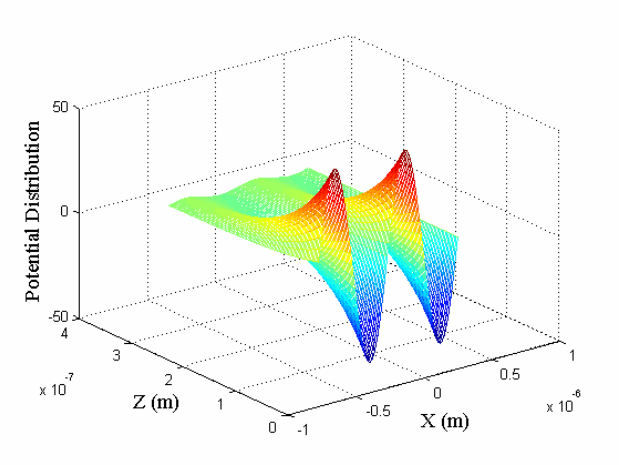

(a)

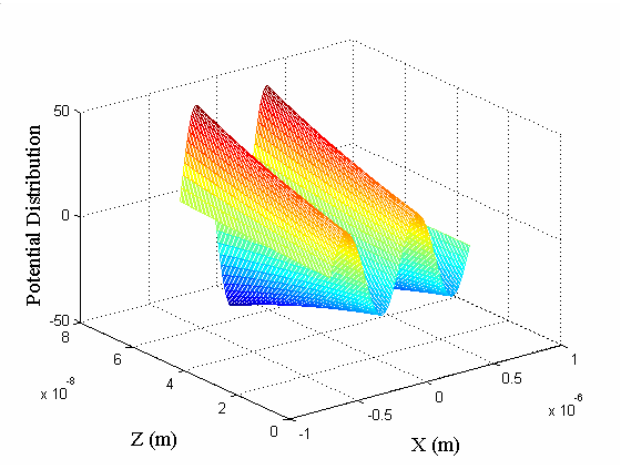

(b)

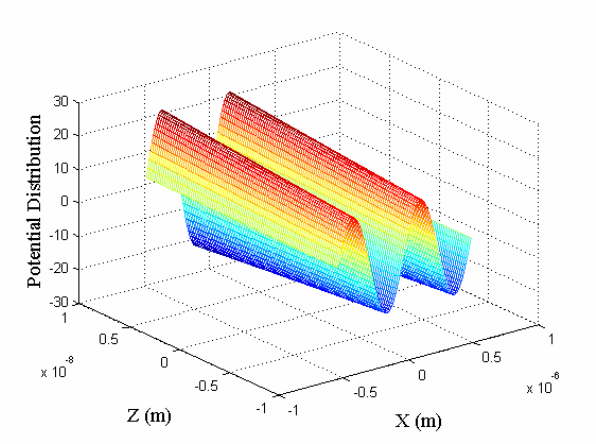

(c)

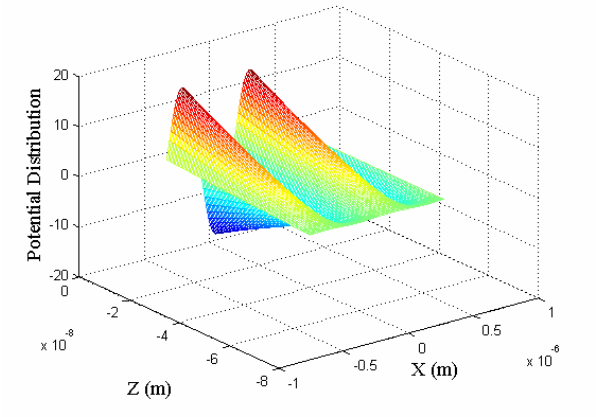

(d)

Figure 4. Potential distribution for equal and non-zero 5 Fourier Components (a) Superstrate region, (b) Upper cladding region, (c) Core region and (d) Lower cladding region ($\varepsilon_{xx}^{Co} = 2.25$, $\varepsilon_{zz}^{Co} = 2.25$, $\varepsilon_{xx}^{Cl} = 2.1025$, $\varepsilon_{zz}^{Cl} = 2.1025$, $V_j = 10$, $d = 3T$).

distributions in different regions.

$$E_x^{(2)}(x,z) = \sum_{j=-N}^{N} -k_j \left[A_j \cosh\left(k_j \delta_2 \left(z - \frac{T}{2}\right)\right) + B_j \sinh\left(k_j \delta_2 \left(z - \frac{T}{2}\right)\right)\right] \cos\left(k_j x\right), \qquad (37)$$

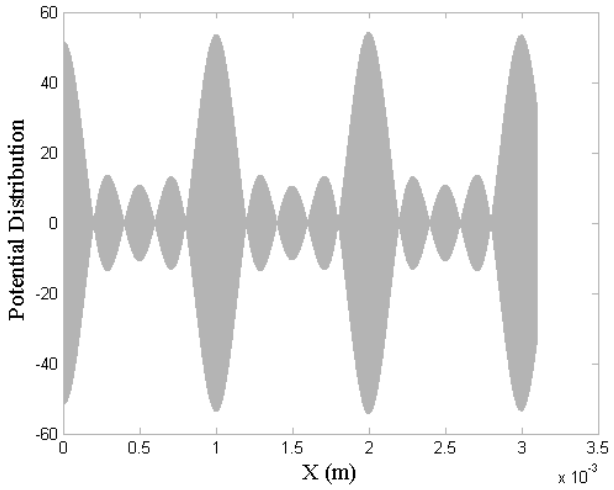

Figure 5. Potential distribution for whole length at $Z = 0$ with same condition in Fig. 3 ($V_j = 10$).

$$E_z^{(2)}(x,z) = \sum_{j=-N}^{N} -\left[A_j k_j \delta_2 \sinh\left(k_j \delta_2 \left(z - \frac{T}{2}\right)\right) + B_j k_j \delta_2 \cosh\left(k_j \delta_2 \left(z - \frac{T}{2}\right)\right)\right] \sin\left(k_j x\right), \tag{38}$$

$$E_x^{(3)}(x,z) = \sum_{j=-N}^{N} -k_j \left[D_j \sinh(k_j \delta_3 z) + E_j \cosh(k_j \delta_3 z)\right] \cos(k_j x), \tag{39}$$

$$E_z^{(3)}(x,z) = \sum_{j=-N}^{N} -[D_j k_j \delta_3 \cosh(k_j \delta_3 z) + E_j k_j \delta_3 \sinh(k_j \delta_3 z)] \sin(k_j x), \tag{40}$$

$$E_x^{(4)}(x,z) = \sum_{j=-N}^{N} -k_j \left[F_j \cosh\left(k_j \delta_2 \left(z + \frac{T}{2}\right)\right) + G_j \sinh\left(k_j \delta_2 \left(z + \frac{T}{2}\right)\right)\right] \cos\left(k_j x\right), \tag{41}$$

$$E_z^{(4)}(x,z) = \sum_{j=-N}^{N} -\left[F_j k_j \delta_2 \sinh\left(k_j \delta_2 \left(z+\frac{T}{2}\right)\right) + G_j k_j \delta_2 \cosh\left(k_j \delta_2 \left(z+\frac{T}{2}\right)\right)\right] \sin\left(k_j x\right). \quad (42)$$

Figure 6 shows the Z-component of the field distribution in the core region.

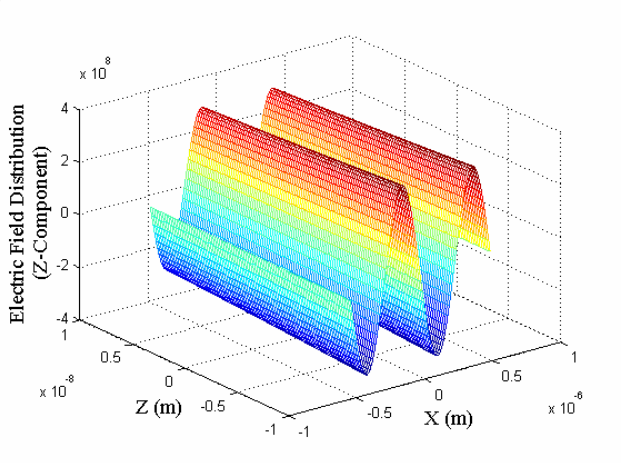

Figure 6. Electric field distribution for core region with same simulating parameters given in Fig. 3 ($V_j = 10$).

Thus, using electro-optical Pockels effect the induced index of refraction can be obtained as follows.

$$\Delta n_{TE}^{(i)} = -\frac{n_{(i)}^3 r_{(i)}^{13}}{2} E_z(x,z), \quad (43)$$

$$\Delta n_{TM}^{(i)} = -\frac{n_{(i)}^3 r_{(i)}^{33}}{2} E_z(x,z), \quad (44)$$

where $r_{(i)}^{13}$ and $r_{(i)}^{33}$ are Pockels EO coefficients [11] for core and cladding regions respectively. Fig. 6 shows the induced index of refraction profile for the core region using $r^{13} = 15 \times 10^{-12}$ V/m.

4. SIMULATION RESULTS AND DISCUSSION

In this section simulated results for the proposed structure both in linear and nonlinear cases are illustrated and discussed. Fig. 8 shows geometrical structure of optical chip for multi wavelength filtering and

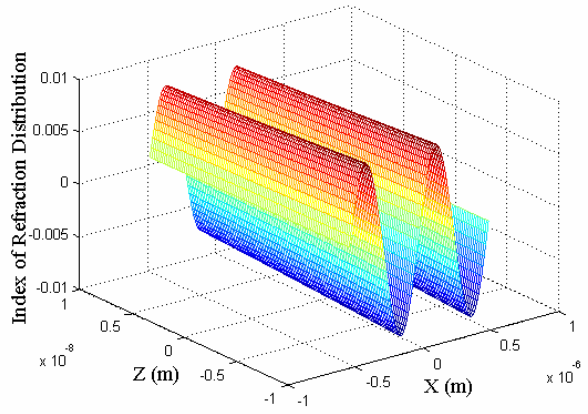

Figure 7. Induced index of refraction distribution in the core region with same simulating parameters given in Fig. 3 and ($r^{13} = 15 \times 10^{-12}$ m/V).

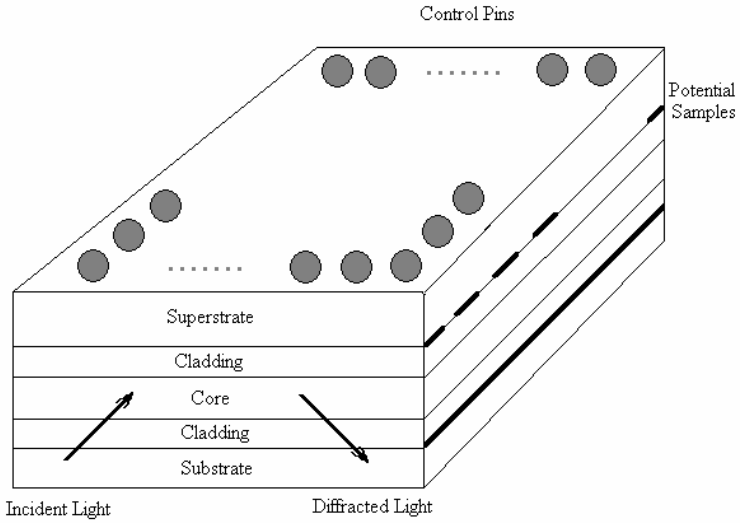

Figure 8. Schematic geometry of the proposed structure.

switching. In this figure gray circles show electrical pads. Fig. 9 shows the refractive index and approximated profile for easy implementation in practice. Approximated case is used for decreasing the number of potential pins.

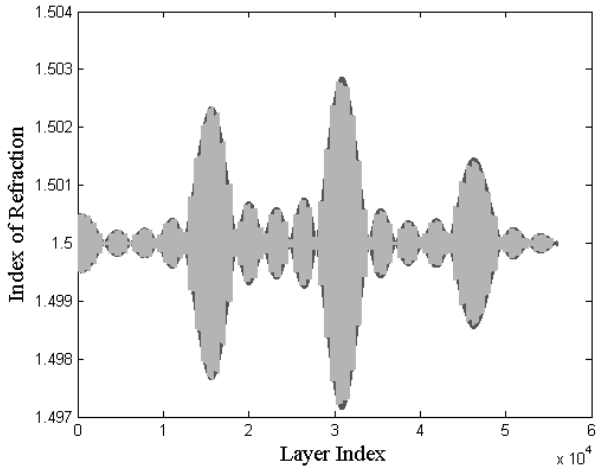

Figure 9. Black: Exact index of refraction profile for manipulation of 5 channels, Gray: Approximated case.

Based on this approximation, the reflection coefficients for 7 and 4 selective similar DWDM channels and 3 channels with different characteristics are shown in Fig. 9 part a, b and c using our proposed approximated method. As it is shown, the approximated cases are acceptable and satisfy practical demand specifications.

Now, as an example, a nonlinear application of the proposed

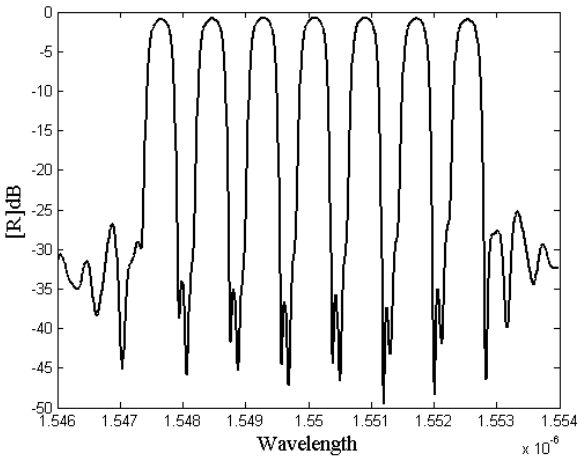

(a)

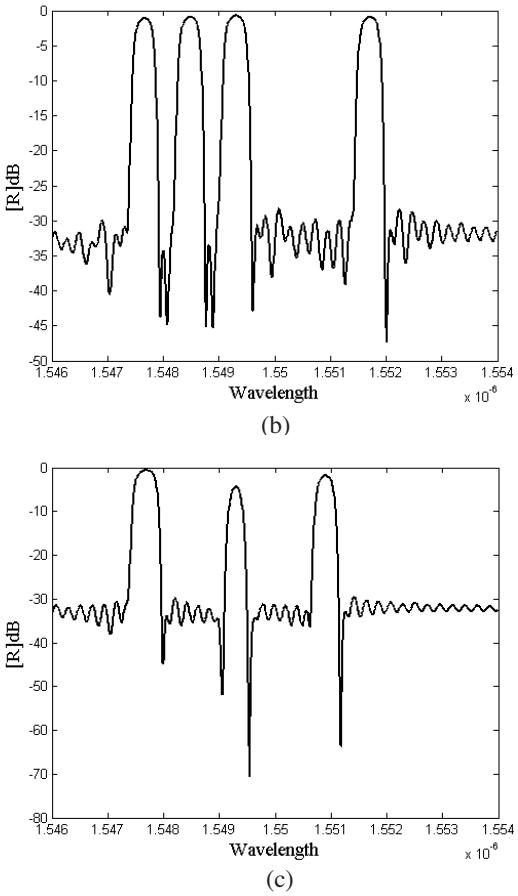

Figure 10. Simulation result using approximated method (a) The reflection coefficient for 7 DWDM channels, (b) for 4 selective channels, and (c) 3 channels with different characteristics.

structure is discussed in the following. For this purpose optical switching is considered. For parameters which are given in the figure caption the following input-output curve in steady state case for different parameters are illustrated. It is shown that for small electric field amplitude the output signal is approximately zero and after a threshold value the output signal is high.

It is shown that with increasing of the nonlinear refractive index coefficient the switching threshold is decreased. Also, using the optical and geometrical parameters used in the proposed structure the switching characteristics can be controlled.

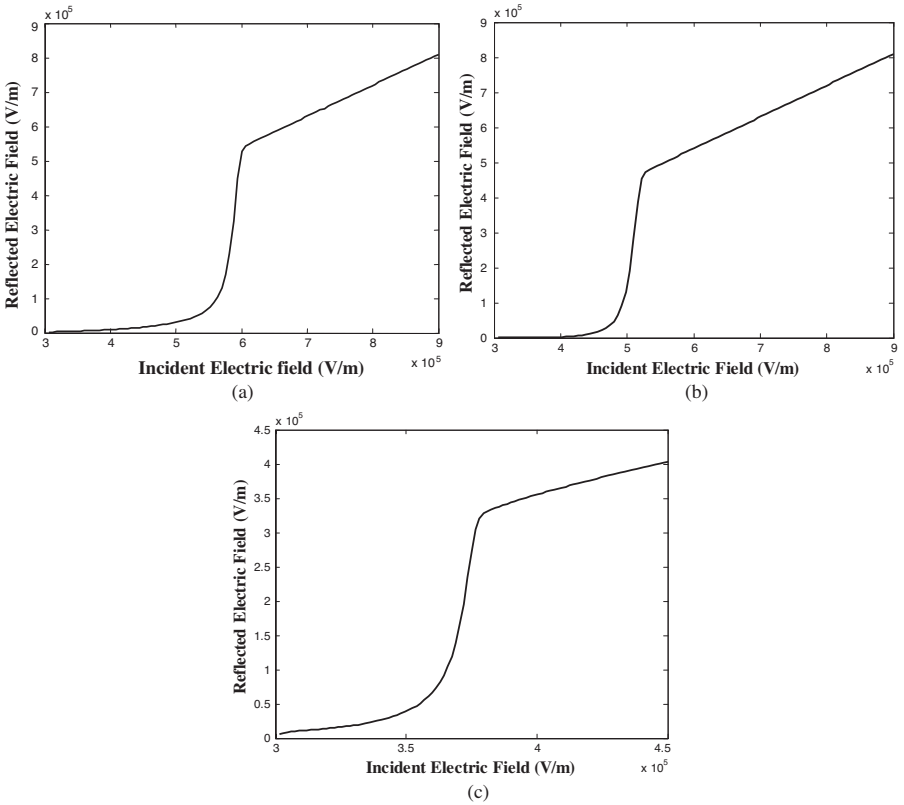

Figure 11. Output electric field Vs. input electric field (a) $L = 1.5\,\text{mm}$, $\delta_{nl} = 1 \times 10^{-13}$, $\delta_l = 0.003$, $n_{ave} = 1$, $\Lambda_3 = 775\,\text{nm}$, (b) $L = 1.5\,\text{mm}$, $\delta_{nl} = 2 \times 10^{-13}$, $\delta_l = 0.003$, $n_{ave} = 1, \Lambda_1 = 775\,\text{nm}$, (c) $L = 1.5\,\text{mm}$, $\delta_{nl} = 5 \times 10^{-13}$, $\delta_l = 0.003$, $n_{ave} = 1$, $\Lambda_2 = 780\,\text{nm}$.

In this section linear and nonlinear applications of the superimposed Bragg Grating were reviewed. We show that using the proposed structure different interesting applications can be obtained.

5. CONCLUSION

In this paper a novel structure for implementation of multi-wavelength optical applications such as optical filtering and switching was introduced. Optical filtering for realization of DWDM standards was discussed. We shown that using the proposed structure different interesting applications can be obtained. Also, a nonlinear application such as optical switching was discussed.

REFERENCES

1. Erdogan, T., "Fiber grating spectra," *J. Lightwave Technology*, Vol. 15, No. 8, Aug. 1997.
2. Zhao, J., X. Shen, and Y. Xia, "Beam splitting, combining, and cross coupling through multiple superimposed volume-index gratings," *Optics & Laser Technology*, Vol. 33, 23–28, 2001.
3. Hruschka, P. C., U. Barabas, and L. Gohler, "Optical narrowband filter without resonances," *Ser.: ELEC. ENERG.*, Vol. 17, 209–217, 2004.
4. Kulishov, M., "Interdigitated electrode-induced phase grating with an electrically switchable and tunable period," *Applied Optics*, Vol. 38, No. 36, 1999.
5. Kulishov, M., "Tunable electro-optic microlense array, I. Planar geometry," *Applied Optics*, Vol. 39, No. 14, 2000.
6. Kulishov, M. and X. Daxhelet, "Electro-optically reconfigurable waveguide superimposed gratings," *Optics Express*, Vol. 9, No. 10, 2001.
7. Kulishov, M., P. Cheben, X. Daxhelet, and S. Delprat, "Electro-optically induced tilted phase gratings in waveguides," *J. Opt. Soc. Am. B*, Vol. 18, No. 4, 2001.
8. Kulishov, M., X. Daxhelet, M. Gaidi, and M. Chaker, "Electronically reconfigurable superimposed waveguide long-period gratings," *J. Opt. Soc. Am. A*, Vol. 19, No. 8, 2002.
9. Kulishov, M., X. Daxhelet, M. Gaidi, and M. Chaker, "Transmission spectrum reconfiguration in long-period gratings electrically induced in pockels-type media with the help of a periodical electrode structure," *J. Lightwave Technology*, Vol. 22, No. 3, 2004.
10. Glytsis, E. N., T. K. Gaylord, and M. G. Moharam, "Electric field, permittivity, and strain distributions induced by interdigitated electrodes on electrooptic waveguides," *J. Lightwave Technology*, Vol. LT-5, No. 5, May 1987.
11. Ramaswami, R. and K. N. Sivarajan, *Optical Networks, A Practical Perspective*, Morgan Kaufmann, San Fransisco, CA, 1998.
12. Roberts, G. F., K. A. Williams, R. V. Penty, I. H. White, M. Glick, D. McAuley, D. J. Kang, and M. Blamire, *Monolithic* 2×2 *Amplifying Add/Drop Switch for Optical Local Area Networking, ECOC '03*, Vol. 3, 736–737, Sept. 24, 2003.
13. Dugan, A., L. Lightworks, and J. C. Chiao, "The optical switching

spectrum: A primer on wavelength switching technologies," *Telecommun. Mag.*, May 2001.

14. Dobbelaere, P. D., K. Falta, L. Fan, S. Gloeckner, and S. Patra, "Digital MEMS for optical switching," *IEEE Commun. Mag.*, 88–95, Mar. 2002.
15. Bregni, S., G. Guerra, and A. Pattavina, "State of the art of optical switching technology for all-optical networks," *Communications World*, WSES Press, Rethymo, Greece, 2001.
16. Mukherjee, B., *Optical Communication Networks*, Mc-Graw-Hill, New York, 1997.
17. Winful, H. G., J. H. Marburger, and E. Garmire, *Appl. Phys. Lett.*, Vol. 35, 379, 1979.
18. Yariv, A., *Quantum Electronics*, John Wiley, 1989.
19. Nishihara, H., M. Haruna, and T. Suhara, *Optical Integrated Circuits*, McGraw-Hill, 1989.
20. Aberg, I., "High-frequency switching and kerr effect — Nonlinear problems solved with nonstationary time domain techniques," *Progress In Electromagnetics Research*, PIER 17, 185–235, 1997.
21. Golmohammadi, S., M. K. Moravvej-Farshi, A. Rostami, and A. Zarifkar, "Spectral analysis of fibonacci-class one-dimensional quasi-periodic structures," *Progress In Electromagnetics Research*, PIER 75, 69–84, 2007.
22. Watanabe, K. and K. Yasumoto, "Two-dimensional electromagnetic scattering of non-plane incident waves by periodic structures," *Progress In Electromagnetics Research*, PIER 74, 241–271, 2007.
23. Khalaj-Amirhosseini, M., "Analysis of periodic and aperiodic coupled nonuniform transmission lines using the fourier series expansion," *Progress In Electromagnetics Research*, PIER 65, 15–26, 2006.
24. Watanabe, K. and K. Kuto, "Numerical analysis of optical waveguides based on periodic fourier transform," *Progress In Electromagnetics Research*, PIER 64, 1–21, 2006.
25. Khalaj-Amirhosseini, M., "Scattering of inhomogeneous two-dimensional periodic dielectric gratings," *Progress In Electromagnetics Research*, PIER 60, 165–177, 2006.
26. Aissaoui, M., J. Zaghdoudi, M. Kanzari, and B. Rezig, "Optical properties of the quasi-periodic one-dimensional generalized multilayer Fibonacci structures," *Progress In Electromagnetics Research*, PIER 59, 69–83, 2006.
27. Zheng, G., A. A. Kishk, A. W. Glisson, and A. B. Yakovlev,

"A novel implementation of modified Maxwell's equations in the periodic finite-difference time-domain method," *Progress In Electromagnetics Research*, PIER 59, 85–100, 2006.

28. Zheng, G., A. A. Kishk, A. W. Glisson, and A. B. Yakovlev, "Implementation of Mur's absorbing boundaries with periodic structures to speed up the design process using finite-difference time-domain method," *Progress In Electromagnetics Research*, PIER 58, 101–114, 2006.
29. Biswas, A., Shwetanshumala, and S. Konar, "Dynamically stable dispersion-managed optical solitons with parabolic law nonlinearity," *J. Electromagnetic Waves and Applications*, Vol. 20, No. 10, 1249–1258, 2006.
30. Maurya, S. N., V. Singh, B. Prasad, and S. P. Ojha, "Modal analysis and waveguide dispersion of an optical waveguide having a cross-section of the shape of a cardioid," *J. Electromagnetic Waves and Applications*, Vol. 20, No. 15, 1021–1035, 2006.
31. Wu, C. J., "Transmission and reflection in a periodic superconductor/dielectric film multilayer structure," *J. Electromagnetic Waves and Applications*, Vol. 19, No. 6, 1991–1996, 2005.